Potential Thermoelectric Performance from Optimization of Hole-Doped Bi_2Se_3

David Parker and David J. Singh

Oak Ridge National Laboratory, 1 Bethel Valley Road, Oak Ridge, Tennessee 37831, USA

(Received 14 July 2011; published 31 October 2011)

We present an analysis of the potential thermoelectric performance of hole-doped Bi_2Se_3, which is commonly considered to show inferior room temperature performance when compared to Bi_2Te_3. We find that if the lattice thermal conductivity can be reduced by nanostructuring techniques (as have been applied to Bi_2Te_3 in Refs. [W. Xie, X. Tang, Y. Yan, Q. Zhang, and T. M. Tritt, *Unique Nanostructures and Enhanced Thermoelectric Performance of Melt-Spun BiSbTe Alloys*, Appl. Phys. Lett. **94**, 102111 (2009); B. Poudel *et al.*, *High-Thermoelectric Performance of Nanostructured Bismuth Antimony Telluride Bulk Alloys*, Science **320**, 634 (2008).]) the material may show optimized ZT values of unity or more in the 300–500 K temperature range and thus be suitable for cooling and moderate temperature waste heat recovery and thermoelectric solar cell applications. Central to this conclusion are the larger band gap and the relatively heavier valence bands of Bi_2Se_3.

DOI: 10.1103/PhysRevX.1.021005 Subject Areas: Energy Research, Semiconductor Physics

I. INTRODUCTION

Good thermoelectric materials are those in which the dimensionless figure-of-merit ZT, defined as

$$ZT = S^2\sigma T/\kappa \tag{1}$$

(where S is the Seebeck coefficient, σ is the electrical conductivity, and κ is the thermal conductivity) approaches or exceeds unity (see Ref. [1] for details of this quantity ZT). In particular, efficient thermoelectric materials could help recover some of the large amounts of energy that are currently wasted in exhaust from fossil fuel combustion. Thermoelectric refrigeration has also received substantial interest as sufficiently efficient devices containing no moving parts could replace the current refrigerant-based cooling devices. See Ref. [2] for a review of this burgeoning field.

Bi_2Te_3 is the thermoelectric that is most commonly used today, and was studied extensively in the 1950s and 1960s when its potential as a thermoelectric material became evident. It can be both electron- and hole-doped—any thermoelectric application requires both types of material—and, when suitably optimized via both the careful tuning of carrier concentration and alloying with Sb and Se, can exhibit a ZT of approximately 1.0 around room temperature. In addition, recent work by the groups of Tritt and Ren [3,4] has demonstrated that ZT values of roughly 1.5 can be obtained in nanostructured Bi_2Te_3. This comes mainly from the reduction of the lattice thermal conductivity without a concomitant reduction in either thermopower S or mobility μ. Bi_2Te_3, however, can only be used in a narrow window around ambient temperature, as its small band gap degrades the thermopower substantially at temperatures above 400 K, while at 200 K ZT has already dropped from unity to 0.5 ([5]).

The sister isostructural rhombohedral material Bi_2Se_3 has received much less attention due largely to its lower mobility, both for electrons and holes, and its somewhat higher lattice thermal conductivity. It is commonly believed not to be a good thermoelectric material for this reason and, indeed, electron-doped Bi_2Se_3 does not appear to be a practical thermoelectric material, as its band masses, and hence Seebeck coefficient, are even lower than those of Bi_2Te_3.

However, the situation is rather different for hole-doped Bi_2Se_3. We will show via our first principles and Boltzmann transport calculations that, due to heavier mass valence bands and accompanying higher density-of-states, hole-doped Bi_2Se_3 has higher low-temperature thermopower than Bi_2Te_3. In addition, the band gap of Bi_2Se_3, at approximately 0.3 eV ([6]), is roughly double that of Bi_2Te_3, so that the thermopower continues to increase at temperatures and carrier concentrations where it is decreasing in Bi_2Te_3. While it is true that the mobility of Bi_2Se_3 is less than that of Bi_2Te_3, this is less of a concern to the extent that the lattice thermal conductivity can be reduced by nanostructuring (as was done for Bi_2Te_3) without reducing the mobility.

In summary, the heavier valence bands and larger band gap—well known to be favorable for thermoelectric performance—mean that nanostructured Bi_2Se_3 may show much better performance than currently believed possible.

To describe what we mean quantitatively, note that the Wiedemann-Franz relation implies that the figure-of-merit ZT can be written as

$$ZT = S^2 r/L_0, \tag{2}$$

where r is the ratio of electronic and total (i.e., electronic + lattice) thermal conductivity, and L_0 is the

Lorenz number, typically near (± 20 percent) the free-electron value of 2.45×10^{-8} $(V/K)^2$ as long as bipolar effects can be neglected. Obviously, if the lattice thermal conductivity term is reduced without a corresponding reduction in the electronic term, higher ZT's will result. Furthermore, at typical temperatures for these heavily doped materials, the lattice term typically decreases as $1/T$, while the electronic term is roughly independent of temperature, so at higher temperatures the ratio r, and hence ZT, will increase. In other words, the lattice thermal conductivity sets the required scale for the mobility, and high mobility is not required if the lattice term is low. This is particularly true if S continues to increase with increasing temperature. We will see that for dopings of interest, this is true for Bi_2Se_3 at temperatures well above 300 K, but is not true for Bi_2Te_3.

II. MODEL, CALCULATED BAND STRUCTURE, AND THERMOPOWER

The results we present below for Bi_2Te_3 and Bi_2Se_3 are based upon our first principles density functional calculations taken within the Perdew-Burke-Ernzerhof generalized gradient approximation combined with Boltzmann transport theory employing the calculated band structure within the constant relaxation time approach. This approach has been used with quantitative accuracy to describe the thermopower of a large number of compounds [7–15], with no fit parameters. It is based upon the observation that electronic scattering times generally do not vary rapidly with energy on a scale of k_BT around the Fermi energy, which is the region important for transport.

We used the WIEN2K [16] code for the electronic structure and the BOLTZTRAP [10] code for the transport calculations. The self-consistent calculations were performed with approximately 2000 k points in the full Brillouin zone (182 in the irreducible wedge for these rhombohedral compounds) with spin-orbit coupling included. The lattice parameters were taken from experiments and the internal coordinates relaxed (without spin-orbit coupling), again with approximately 2000 k points. The transport calculations were performed with approximately 30 000 k points in the full Brillouin zone; these results did not vary significantly from those performed with 10 000 k points so that proper convergence was attained. We also use the constant relaxation time approach to include a calculation of the appropriate Lorenz number relating electrical conductivity and electronic thermal conductivity to use in the estimation of ZT (Sec. IV). As with the thermopower, the Lorenz number is expressed as ratios of transport integrals (see Ref. [5] for the actual expression) and can therefore be calculated with no adjustable parameters under the assumption of a constant relaxation time. Use of the actual Lorenz number helps to properly characterize bipolar thermal conduction—an important issue at moderate temperatures (~ 500 K) for this small band gap semiconductor. We will see that the main impact of using this Lorenz number is that, at 500 K, slightly heavier dopings (farther from the bipolar regime) yield optimal performance.

With regards to the constant relaxation time approximation, a brief discussion is in order. We restrict ourselves to a discussion of the use of this assumption in calculating the thermopower, as the calculation for the Lorenz number is very similar. The canonical expressions for the thermopower $S(T)$ and the related quantity, the conductivity $\sigma(T)$, are as follows [note that $-\mathrm{sech}^2(x) = 4df/dx$, f the Fermi function]:

$$S(T) = \frac{\int_{-\infty}^{\infty} dE\sigma(E)(E-\mu)\partial f/\partial E}{T\int_{-\infty}^{\infty} dE\sigma(E)\partial f/\partial E}, \tag{3}$$

$$\sigma(T) = -\int_{-\infty}^{\infty} dE\sigma(E)\partial f/\partial E, \tag{4}$$

$$\sigma(E) = N(E)v^2(E)\tau(E), \tag{5}$$

where $\tau(E)$ is the scattering time, $v(E)$ is the Fermi velocity, and $N(E)$ is the density-of-states. We have suppressed the tensor indices, and note that the integrations in reality involve a Brillouin-zone sum of the quantity $\sigma_k = N(k)v_k^2\tau_k$ for energy eigenvalues $\epsilon_k = E$. An inspection of these equations reveals that the relaxation time $\tau(E)$ is present both in the integral in the numerator of $S(T)$ [Eq. (3)] and in the electrical conductivity $\sigma(T)$ in the denominator, convoluted with the derivative of the Fermi function, which has half width at half maximum slightly larger than kT. Therefore, if the scattering rate $\tau(E)$ does not vary substantially on this energy scale, it is effectively constant over the important region of integration and simply cancels out. Note that we are not making an assumption regarding $\tau(E)$ being constant with the temperature T. Temperature can and does affect the absolute value of the electronic scattering time—but for the thermopower this absolute value is of no importance.

We note also that the types of nanostructuring assumed here, as were considered in Refs. [3,4], are generally of dimensions intermediate between bulk electronic and phononic mean free paths, so that while the *phonon* mean free path would be shortened, reducing the lattice thermal conductivity, the electron mean free path would not likely be altered substantially. Therefore, the electron relaxation time would not be affected by the nanostructuring. We are explicitly here not considering quantum-well–type nanostructures of small (~ 10 Å) dimensions, which could affect relaxation times.

As described previously, the constant scattering time approximation has been used with considerable success in the last decade. Recent successes include the prediction [9] and experimental verification [17] of PbSe as a good high-temperature thermoelectric material. Also, it was predicted [18] that PbTe performance could be enhanced by

appropriate doping with elements other than Tl (Tl-doped PbTe was previously known as a high performance material whose properties were claimed to be due to resonant enhancement associated with Tl chemistry) [19]. One area where this approximation can yield errors is in situations where bipolar conduction is prevalent, where electron-to-hole mobility ratios can outstrip band mass differences. However, in these situations thermoelectric performance is generally reduced radically and so these situations are usually of little interest. Finally, we note parenthetically that in the case of acoustic phonon-electronic scattering, $\tau(E)$ is sometimes assumed to be $\propto (E - E_0)^{-0.5}$ [1], where E_0 is the energy of the band edge. This will, in general, reduce the thermopower slightly, but will also tend to reduce the value of the Lorenz number (for all but the fully degenerate limit), so that the effect on ultimate thermoelectric performance is unclear. Given this and the value of simplicity, as well as the many successes of the constant scattering time approximation, we have opted to retain this approximation throughout this paper.

Considerable research has been done regarding the effects of nanostructuring (specifically, superlattices) on the figure-of-merit ZT [20–30]. These works have generally found that such superlattices, by virtue of the sharpening of the density-of-states caused in a small scale system, can attain substantial increases in ZT. Substantial increases in thermopower have been predicted and observed for such superlattices. In addition, some work has indicated similar effects for small-grain nanostructuring [23]. However, we are specifically not studying superlattices here as the feasibility of scaling up such systems remains an open question. As far as the electronic filtering effects proposed in Refs. [21,23], such effects may be relevant here, and generally act to increase the thermopower, while we assume no such increase. Conversely, we make no assumption of decreased electron mobility due to nanostructuring, while recent data [3,4] indicate that some reduction may occur. These two neglected effects will tend to oppose each other, so that the final performance (ZT) predictions are likely to be reasonable ones.

As mentioned previously, both compounds form in the rhombohedral structure, space group 166, R-3 m. The unit cell is roughly 20% larger for the Te compound than for that of Se; there are five atoms in the unit cell.

Presented in Fig. 1 are the calculated band structures of Bi_2Se_3 and Bi_2Te_3. We note two salient features. First, the band gap of Bi_2Se_3, calculated at 0.26 eV, is some 70% larger than the Bi_2Te_3 band gap of 0.15 eV. As noted previously by Ioffe, Nolas, and Goldsmid, [1,5], the larger band gap greatly reduces the effects of bipolar conduction, which is always negative for thermoelectric performance. Experimentally, the Bi_2Se_3 band gap is slightly larger, at approximately 0.3–0.35 eV, which means that some of our results may slightly understate the performance of Bi_2Se_3, while the Bi_2Te_3 gap is roughly correct. The second

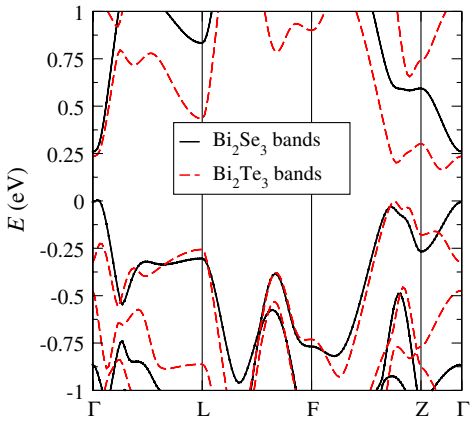

FIG. 1. The calculated band structure for Bi_2Se_3 and Bi_2Te_3 in the rhombohedral Brillouin zone. The valence band maximum is set to the energy zero.

prominent feature is the existence of a Γ-centered valence band local maximum for Bi_2Se_3 in addition to the maximum between F and Z, which is present for both materials. This feature ensures higher carrier concentration at a given thermopower for Bi_2Se_3 relative to Bi_2Te_3, or, equivalently, higher thermopower at a given carrier concentration. We note parenthetically that exactly the opposite is true for the conduction bands, where it is Bi_2Te_3 that has the additional minimum, as well as a less dispersive band, and will consequently show higher thermopower. Here we focus on hole-doped Bi_2Se_3. The band masses for the relevant valence bands are as follows: For Bi_2Se_3, the valence band maximum (VBM) at the Γ point has a fairly anisotropic mass of 0.67 m_0 (m_0 is the free-electron mass) in the c-axis direction and 0.38 m_0 in-plane. This last value is somewhat larger than some literature values but is, in fact, rather consistent with ARPES data from Ref. [6]. For the maximum located on the F-Z symmetry axis, the pocket is also anisotropic, with mass on the F side of the pocket of 0.29 m_0 and 1.33 m_0 on the Z side. For the Bi_2Te_3 VBM, located in largely the same momentum space location as the near-VBM of Bi_2Se_3, the corresponding values are 0.28 m_0 and 1.45 m_0, which are very similar to the Bi_2Se_3 masses. It is the additional Γ-centered VBM that is ultimately responsible for the favorable thermopower behavior of Bi_2Se_3, so that it is perhaps more accurate to speak of the convergence of band maxima [31], rather than the actual band mass, as the origin of the enhanced thermopower.

We should mention that in actual fact, p-type Bi_2Te_3 is an alloyed combination of 75% Sb_2Te_3 and 25% Bi_2Te_3. However, the band structure of Sb_2Te_3 is similar to that of Bi_2Te_3, and the actual performance of this p-type material is very similar to that of the n-type material (for which much less alloying is used), so that the comparison of the thermoelectric performance between Bi_2Se_3 and Bi_2Te_3 remains valid.

We have plotted in Fig. 2 the density-of-states for both compounds. As is apparent, the density-of-states increases more quickly for Bi_2Se_3 than for Bi_2Te_3, which will lead to larger thermopower. Note that the unit cell of Bi_2Te_3 is some 20% larger than that of Bi_2Se_3, so on a volume basis the disparity in the density-of-states is even larger. We make this point because the units of carrier concentration that are relevant for experiments are on a volume basis (i.e., cm^{-3}), as we are looking for high thermopower at high carrier concentration, where the electrical conduction is heightened.

In Fig. 3 we present the calculated thermopower at 300 K for both compounds, both in the planar (ab) and c-axis directions. As expected, the thermopower is significantly higher for Bi_2Se_3, particularly in the neighborhood of 10^{19}–10^{20} cm^{-3}, where thermoelectric performance is near to optimum for these compounds. In this range the Bi_2Se_3 thermopower is 30% to 50% greater than for Bi_2Te_3. We note also that in this range of carrier concentration the Bi_2Se_3 thermopower does not saturate, as does the Bi_2Te_3—a direct result of the larger band gap of Bi_2Se_3.

We note that for Bi_2Se_3, the calculated planar thermopower at $T = 300$ K and hole concentration $p = 10^{19}$ cm^{-3} is approximately 380 μV/K. This is substantially larger than that measured by Cava's group, where the carrier concentration was determined from Hall measurements as 10^{19} cm^{-3}. However, this is virtually the first study to succeed in the hole doping of Bi_2Se_3, and may not represent an accurate value of the carrier concentration. This is particularly true in view of the use of the highly reactive calcium as the dopant in this study—carrier concentration is likely very difficult to control with this dopant. We expect that future studies building upon the experience of this first hole-doping study will show thermopowers more in line with our predictions.

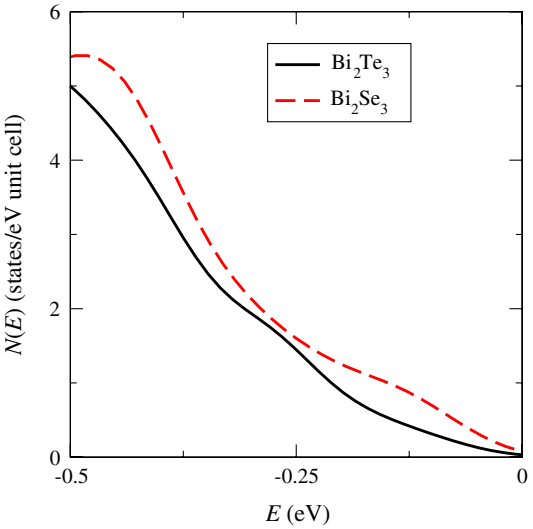

FIG. 2. The calculated density-of-states for the valence bands of Bi_2Se_3 and Bi_2Te_3. Note the larger values for Bi_2Se_3 just below the valence band maximum, particularly in the first quarter eV—the most important region for temperatures below 500 K. For both compounds, the valence band maximum is set to the energy zero.

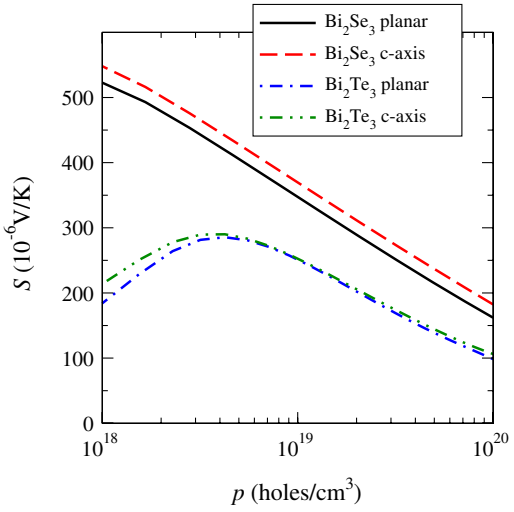

FIG. 3. The calculated thermopower for Bi_2Se_3 and Bi_2Te_3 at 300 K.

Figure 4 depicts the calculated thermopower at 500 K for both compounds, as before, in both directions. Here the advantages of Bi_2Se_3 are even more apparent, with a peak thermpower over 400 μV/K for a carrier concentration of $10^{19}/cm^3$. The corresponding maximum for Bi_2Te_3 is only 225 μV/K, and at this carrier concentration Bi_2Se_3's thermopower is roughly 50% greater. This is of interest for certain solar thermoelectric applications [32], which operate in this temperature range. Most notably, the effects of bipolar conduction—evident as a decrease in thermopower at decreasing carrier concentration—are not apparent for

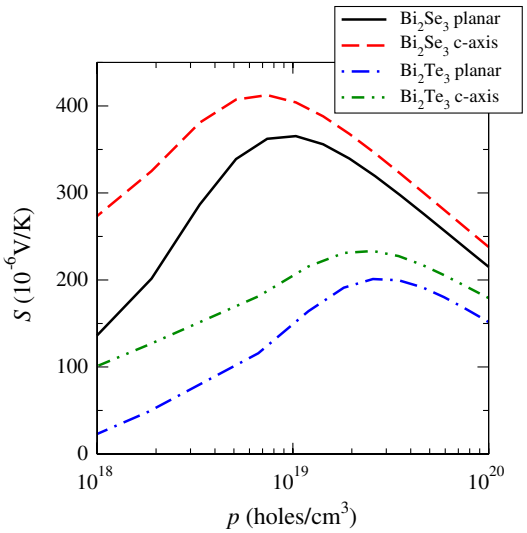

FIG. 4. The calculated thermopower for Bi_2Se_3 and Bi_2Te_3 at 500 K.

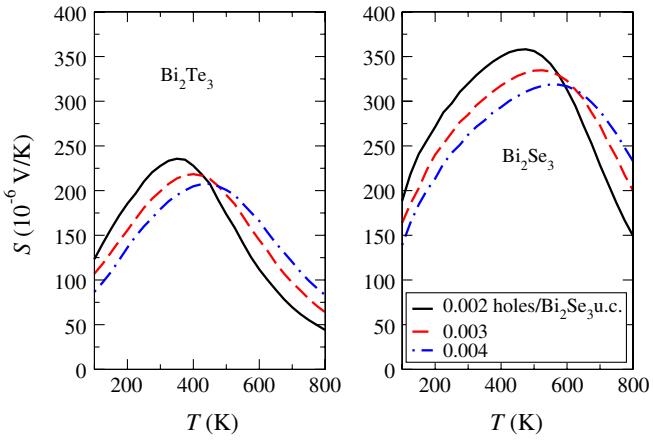

FIG. 5. The calculated thermopower for Bi_2Se_3 and Bi_2Te_3 at the indicated carrier concentrations. Lines of the same color and character have equal carrier concentrations.

Bi_2Se_3 until below $10^{19}/cm^3$, while this regime begins at $3 \times 10^{19}/cm^3$ for Bi_2Te_3. The bipolar regime is doubly destructive for thermoelectric performance because, in addition to decreasing thermopower, it creates the bipolar thermal conductivity, which can greatly increase the Lorenz number in Eq. (2) and thereby greatly reduce thermoelectric performance (i.e., ZT), and this begins at slightly lower temperatures than does the maximum in the thermopower.

To make the point about temperature dependence even more explicit, in Fig. 5 we present temperature dependence results at fixed carrier concentration. The Bi_2Se_3 thermopower is larger for all temperatures and dopings, and exhibits a maximum roughly 50% higher than that of Bi_2Te_3. In addition, this maximum is at significantly higher temperatures—500 to 600 K for Bi_2Se_3 as opposed to 300 to 400 K for Bi_2Te_3. In this temperature range, the lattice thermal conductivity is expected to be proportional to $1/T$, while the electronic thermal conductivity (assuming one avoids the bipolar regime) is roughly constant. This suggests that the best performance of Bi_2Se_3 is likely to be found in the 400–600 K range, although we still expect that good performance will be obtained at ambient temperature, as refrigeration applications would require. In the following section, we make estimates of the potential performance of Bi_2Se_3 in these temperature ranges, and, in addition, specify estimates of carrier concentration where optimal performance may be found.

III. ACCURACY OF RIGID BAND AND DOPING FEASIBILITY ASSUMPTIONS

As stated above, for this study we have assumed rigid bands in which the effect of dopants is modeled as simply adding or removing charge from the system—it is assumed that only the Fermi level, not the band *shape*, changes with doping. It can be argued that this assumption could break down for small band gap semiconductors, as studied here; in addition, the thermopower is highly sensitive to the exact shape of the density-of-states near the band edge, so it is possible that simply adding or subtracting charge is not an accurate depiction of the behavior of the system.

To assess this possibility, we have performed additional band structure calculations within the virtual crystal approximation, separately modeling hole doping on both the Bi (as doping with lead would produce) and Se (as doping with arsenic would produce) sites, and computed the density-of-states. We present the results of these calculations in Fig. 6. The virtual crystal approximation is an average potential approximation that gives results different from the rigid band approximation when the band structure is sensitive to alloying. As shown, this is not the case here, supporting the treatment that we use. (Alloys are sometimes treated with the coherent potential approximation, which differs from the VCA in that it is an average

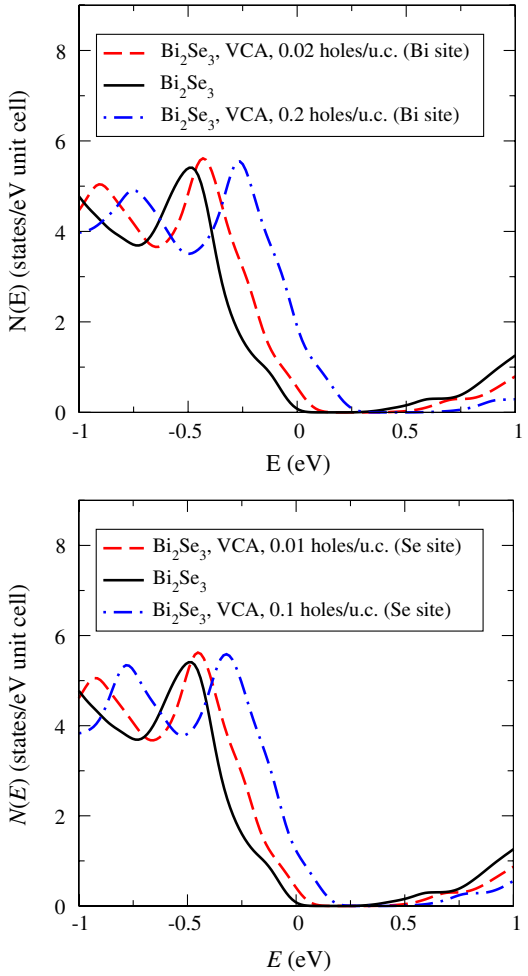

FIG. 6. Shown are the effects on the calculated Bi_2Se_3 density-of-states of doping on the Bi site (top), and Se site (bottom), for the indicated doping levels within the virtual crystal approximation. In both cases the valence band maximum of Bi_2Se_3 is set to the energy zero.

scattering approximation. This could be used to look at disorder-induced band tails, for example.)

As indicated in the plots, for doping ranges of 0.01–0.02 holes per unit cell, the density-of-states in the first 0.5 eV below the VBM is essentially identical to that of the pure compound, so that the thermopower will show the same behavior. Slightly larger variations can be discerned for the larger doping ranges of 0.1–0.2 holes per unit cell, but as described in the following section, these dopings are far larger than would be used to determine optimal thermoelectric performance. One can also perform more involved coherent potential approximation calculations, but these are impractical and likely unnecessary for the small dopings of this study. We conclude that for the dopings of interest studied here the rigid band approximation can be trusted to give reliable results.

Note that we have not attempted to determine via first principles calculations any thermodynamic stability of the dopings studied here. However, it is highly likely that the doping ranges modeled here (as detailed in the next section, of between 0.001 and 0.006 holes per unit cell) will be achievable in practice. First, the work of Cava's group achieved 300 K dopings given as 10^{19} cm^{-3}, or roughly 0.0015 holes per unit cell, and these may be understated, given the lower than expected thermopower at these concentrations. Additionally, samples with larger Ca content (whose carrier concentration was not measured) showed lower thermopower, indicative of still higher hole concentrations. Given that the melting point of Bi_2Se_3 is nearly 1000 K, it is rather unlikely that thermal effects would cause this level of dopant to be unstable at 500 K. Finally, we note that the sister isostructural and isoelectronic material Bi_2Te_3 is easily dopable to this range of carrier concentration and temperature without difficulty. For all these reasons we expect Bi_2Se_3 to be readily dopable to the concentration ranges relevant for thermoelectric performance.

IV. CALCULATION OF OPTIMAL DOPING RANGES AND POTENTIAL PERFORMANCE

The discussion in the Introduction makes clear that the potential thermoelectric performance will depend sensitively upon the lattice thermal conductivity, which can be reduced to an extent by nanostructuring. In an attempt to estimate this performance, we present in Figs. 7 and 8, the calculated values of ZT at 300 and 500 K, respectively, under two separate scenarios. The first one takes the 300 K lattice thermal conductivity as that of bulk Bi_2Se_3, given in Ref. [5], as approximately 2 W/m K. The second one assumes that via alloying and nanostructuring, the 300 K lattice term is reduced to 0.5 W/m K. While such a reduction may seem optimistic, in the cited Bi_2Te_3 work the lattice term after melt spinning was estimated at less than 0.3 W/m K. Note that for Fig. 8 we have assumed equivalent scenarios to that of Fig. 7, but have assumed that the

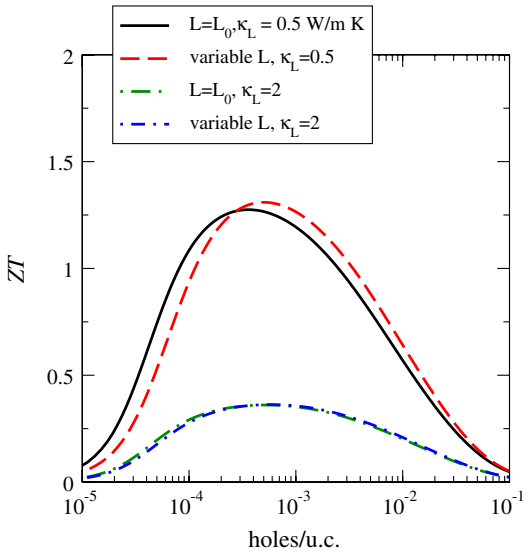

FIG. 7. The calculated figure-of-merit ZT for Bi_2Se_3 at 300 K, for the indicated 300 K values of the lattice thermal conductivity, and with the free-electron Lorenz number of 2.45×10^{-8} (V/K)^2 as well as that calculated from the first principles approach. Note that one hole per unit cell is 7.08×10^{21}/cm^3.

lattice term and mobility obey a $1/T$ law for both scenarios, with the exception of the nanostructured lattice term at 500 K (described below).

For the carrier concentration dependence of the mobility, we have simply assumed that $\mu \propto p^{-0.6}$, as in another recently published work [9], and used the measured mobility of approximately 130 cm^2/V-sec at a carrier concentration $p = 10^{19}$ cm^{-3} from the work of Cava's group [6] on single crystal p-type Bi_2Se_3. This is the main recently published work on p-type Bi_2Se_3; a previous

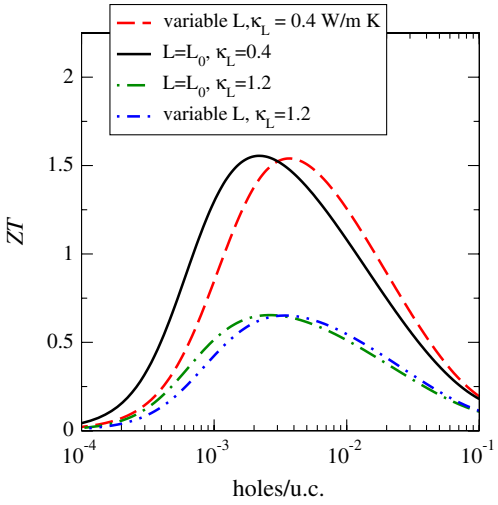

FIG. 8. The calculated figure-of-merit ZT for Bi_2Se_3 at 500 K, for the indicated 500 K values of the lattice thermal conductivity, and with the free-electron Lorenz number as well as the first principles calculated value.

work [33] found a mobility of 175 $cm^2/V\text{-}sec$ at essentially the same carrier concentration. An earlier work on much more lightly doped p-type samples [34] found substantially higher mobilities, so the assumption that mobility increases at these concentrations is a reasonable one. Bi_2Se_3 ordinarily forms n-type specimens, so that more literature on n-type is available. Typical n-type mobilities at or even somewhat above these concentrations [35–41] are in this range or higher, so that assuming no great asymmetry in n-type vs p-type scattering rates, the assumed p-type mobilities are reasonable. The assumed carrier concentration dependence implies that mobility increases significantly as carrier concentration decreases, which is generally true until one reaches a limiting value, as in Ref. [42]. Given the general lack of data regarding p-type mobility doping dependence in this material, this implies that our results at low carrier concentration, where we assume increased mobility, contain some uncertainty.

With this discussion completed, we now turn to our ZT estimates. We begin with the 300 K results in Fig. 7. As one might expect, at this temperature the effects of allowing the Lorenz number to deviate from its free-electron value are rather small. For the $\kappa_{\text{lattice}} = 2\ \text{W/m K}$, we find a maximum figure-of-merit of approximately 0.35, at a carrier concentration of approximately 0.001 holes per unit cell, or $7 \times 10^{18}\ \text{cm}^{-3}$. While this may seem unimpressive, one must remember that even Bi_2Te_3, the prototypical thermoelectric material, only has a maximum ZT of 0.6 without alloying optimization—it is largely the reduction in κ_{lattice} by alloying that allows one to attain ZT values of unity at room temperature. When this effect (including alloying and nanostructuring) is taken into account and a much smaller κ_{lattice} of 0.5 W/m K is assumed, one finds, unsurprisingly, much larger values of ZT, with a maximum value of roughly 1.3 at the same carrier concentration as without the lattice thermal conductivity. Such a value, if confirmed experimentally, would place Bi_2Se_3 as a viable, cost effective replacement for Bi_2Te_3 in thermoelectric cooling applications.

The 500 K results are depicted in Fig. 8. Somewhat larger effects of using the first principles Lorenz number are apparent, and, in addition, the optimal carrier concentrations are somewhat larger than at 300 K due to the need to minimize the effects of bipolar thermal conduction, which is much more of a concern at the higher temperature. Maximum ZT values are found for concentrations between 0.003 and 0.006 holes per unit cell, or $2 - 4 \times 10^{19}\ \text{cm}^{-3}$, with the maximum ZT value assuming the larger 500 K κ_{lattice} of 1.2 W/m K of approximately 0.7 and the ZT value at the lower κ_{lattice} of 0.4 W/m K attaining approximately 1.5. The higher value, if confirmed, would place Bi_2Se_3 among the best known materials in the 500 K range. Note that while we have assumed a $1/T$ relationship for the lattice thermal conductivity for the non-nanostructured case, we have not done this for the nanostructured case as it is plausible that such materials may approach the "minimum thermal conductivity" [43], where the phonon mean free path is of order one unit cell length. We have therefore assumed only a modest κ_{lattice} decrease (from 0.5 to 0.4 W/m K) in the nanostructured case as the temperature is increased from 300 to 500 K.

V. DISCUSSION AND SUMMARY

As indicated previously, despite being a sister material to the well-known Bi_2Te_3, Bi_2Se_3 has undergone much less consideration as a thermoelectric material, and very little thermoelectric data has been taken for hole dopings. Given the scarcity of Te, finding Bi_2Te_3 alternatives, as attempted in this work, is of importance for practical applications, and we hope that the present work spurs study of hole-doped Bi_2Se_3. As in other recent work, the doping dependence of the mobility—particularly, at the low carrier concentrations indicated as optimal at 300 K—is a major unknown in this analysis, and could significantly affect the quantitative conclusions made regarding ZT and its doping dependence. An additional unknown is what level of lattice thermal conductivity reduction is practical for this material. What will remain unchanged, however, is the following:

(i) Bi_2Se_3, by virtue of its larger band gap and heavier valence band, will yield p-type performance superior to Bi_2Te_3 in the moderate temperature range 400–600 K.

(ii) Optimization of Bi_2Se_3, by optimizing carrier concentration, alloying, and nanostructuring, can be expected to yield ZT performance, which substantially exceeds the current expectations for this material.

ACKNOWLEDGMENTS

We thank Jiong Yang, Wenqing Zhang, and Zhifeng Ren for useful discussions. This research was supported by the U.S. Department of Energy, EERE, Vehicle Technologies, Propulsion Materials Program (D. P.), and the Solid State Solar-Thermal Energy Conversion Center (S3 TEC), an Energy Frontier Research Center funded by the U.S. Department of Energy, Office of Science, Office of Basic Energy Sciences under Contract No. DE-SC0001299/DE-FG02-09ER46577 (D. J. S.).

[1] A. F. Ioffe, *Semiconductor Thermoelements and Thermoelectric Cooling* (Inforesearch, London, 1957).

[2] Special Issue: International Conference on Thermoelectrics 2010, edited by L. Chen, J. Yang, H. Böttner, D. T. Morelli, and R. Funahashi [J. Electron. Mater. **40**, 479 (2011)].

[3] W. Xie, X. Tang, Y. Yan, Q. Zhang, and T. M. Tritt, *Unique Nanostructures and Enhanced Thermoelectric*

Performance of Melt-Spun BiSbTe Alloys, Appl. Phys. Lett. **94**, 102111 (2009).

[4] B. Poudel, Q. Hao, Y. Ma, Y. Lan, A. Minnich, B. Yu, X. Yan, D. Wang, A. Muto, D. Vashaee, X. Chen, J. Liu, M. S. Dresselhaus, G. Chen, and Z. Ren, *High-Thermoelectric Performance of Nanostructured Bismuth Antimony Telluride Bulk Alloys*, Science **320**, 634 (2008).

[5] G. S Nolas, J. Sharp, and H. J. Goldsmid, *Thermoelectrics* (Springer, Berlin 2001).

[6] Y. S. Hor, A. Richardella, P. Roushan, Y. Xia, J. G. Checkelsky, A. Yazdani, M. Z. Hasan, N. P. Ong, and R. J. Cava, *p-Type* Bi_2Se_3 *for Topological Insulator and Low-Temperature Thermoelectric Applications*, Phys. Rev. B **79**, 195208 (2009).

[7] L. Zhang, M.-H. Du, and D. J. Singh, *Zintl-Phase Compounds with* $SnSb_4$ *Tetrahedral Anions: Electronic Structure and Thermoelectric Properties*, Phys. Rev. B **81**, 075117 (2010).

[8] D. J. Singh, *Electronic and Thermoelectric Properties of* $CuCoO_2$*: Density Functional Calculations*, Phys. Rev. B **76**, 085110 (2007).

[9] D. Parker and D. J. Singh, *High-Temperature Thermoelectric Performance of Heavily Doped PbSe*, Phys. Rev. B **82**, 035204 (2010).

[10] G. K. H. Madsen, K. Schwarz, P. Blaha, and D. J. Singh, *Electronic Structure and Transport in Type-I and Type-VIII Clathrates Containing Strontium, Barium, and Europium*, Phys. Rev. B **68**, 125212 (2003).

[11] D. J. Singh and I. I. Mazin, *Calculated Thermoelectric Properties of La-Filled Skutterudites*, Phys. Rev. B **56**, R1650 (1997).

[12] T. J. Scheidemantel, C. Ambrosch-Draxl, T. Thonhauser, J. V. Badding, and J. O. Sofo, *Transport Coefficients from First-Principles Calculations*, Phys. Rev. B **68**, 125210 (2003).

[13] L. Bertini and C. Gatti, *The Impact of the Actual Geometrical Structure of a Thermoelectric Material on its Electronic Transport Properties: The Case of Doped Skutterudite Systems*, J. Chem. Phys. **121**, 8983 (2004).

[14] L. Lykke, B. B. Iversen, and G. K. H. Madsen, *Electronic Structure and Transport in the Low-Temperature Thermoelectric* $CsBi_4Te_6$*: Semiclassical Transport Equations*, Phys. Rev. B **73**, 195121 (2006).

[15] Y. Wang, X. Chen, T. Cui, Y. Niu, Y. Wang, M. Wang, Y. Ma, and G. Zou, *Enhanced Thermoelectric Performance of PbTe within the Orthorhombic Pnma Phase*, Phys. Rev. B **76**, 155127 (2007).

[16] P. Blaha, K. Schwarz, G. K. H. Madsen, D. Kvasnicka, and J. Luitz, WIEN2K, An Augmented Plane Wave + Local Orbitals Program for Calculating Crystal Properties (Karlheinz Schwarz, Techn. Universität Wien, Austria, 2001), ISBN 3-9501031-1-2.

[17] H. Wang, Y. Pei, A. D. LaLonde and G. J. Snyder, *Heavily Doped p-Type PbSe with High Thermoelectric Performance: An Alternative for PbTe*, Adv. Mater. **23**, 1366 (2011).

[18] D. J. Singh, *Doping-Dependent Thermopower of PbTe from Boltzmann Transport Calculations*, Phys. Rev. B **81**, 195217 (2010).

[19] J. P. Heremans, V. Jovovic, E. S. Toberer, A. Saramat, K. Kurosaki, A. Charoenphakdee, S. Yamanaka, and G. J. Snyder, *Enhancement of Thermoelectric Efficiency in PbTe by Distortion of the Electronic Density of States*, Science **321**, 554 (2008).

[20] Y. Q. Cao, X. B. Zhao, T. J. Zhu, X. B. Zhang, and J. P. Tu, *Syntheses and Thermoelectric Properties of Bi2Te3/Sb2Te3 Bulk Nanocomposites with Laminated Nanostructure*, Appl. Phys. Lett. **92**, 143106 (2008).

[21] J. M. O. Zide, D. Vashaee, Z. X. Bian, G. Zeng, J. E. Bowers, A. Shakouri, and A. C. Gossard, *Demonstration of Electron Filtering to Increase the Seebeck Coefficient in* $In_{0.53}Ga_{0.47}As/In_{0.53}Ga_{0.28}Al_{0.19}As$ *Superlattices*, Phys. Rev. B **74**, 205335 (2006).

[22] G. Chen and M. Neagu, *Thermal Conductivity and Heat Transfer in Superlattices*, Appl. Phys. Lett. **71**, 2761 (1997).

[23] J. P. Heremans, C. M. Thrush, and D. T. Morelli, *Thermopower Enhancement in Lead Telluride Nanostructures*, Phys. Rev. B **70**, 115334 (2004).

[24] G. Chen, *Thermal Conductivity and Ballistic-Phonon Transport in the Cross-Plane Direction of Superlattices*, Phys. Rev. B **57**, 14958 (1998).

[25] L. D. Hicks, T. C. Harman, and M. S. Dresselhaus, *Use of Quantum-Well Superlattices to Obtain a High Figure of Merit from Nonconventional Thermoelectric Materials*, Appl. Phys. Lett. **63**, 3230 (1993).

[26] L. D. Hicks and M. S. Dresselhaus, *Effect of Quantum-Well Structures on the Thermoelectric Figure of Merit*, Phys. Rev. B **47**, 12727 (1993).

[27] R. Venkatasubramanian, *Lattice Thermal Conductivity Reduction and Phonon Localizationlike Behavior in Superlattice Structures*, Phys. Rev. B **61**, 3091 (2000).

[28] D. A. Broido and T. L. Reinecke, *Effect of Superlattice Structure on the Thermoelectric Figure of Merit*, Phys. Rev. B **51**, 13797 (1995).

[29] R. Venkatasubramanian, E. Siivola, T. Colpitts and B. O'Quinn, *Thin-Film Thermoelectric Devices with High Room-Temperature Figures of Merit*, Nature (London) **413**, 597 (2001).

[30] J. Zhou, C. Jin, J. H. Seo, X. Li, and L. Shi, *Thermoelectric Properties of Individual Electrodeposited Bismuth Telluride Nanowires*, Appl. Phys. Lett. **87**, 133109 (2005).

[31] Y. Pei, X. Shi, A. LaLonde, H. Wang, L. Chen, and G. J. Snyder, *Convergence of Electronic Bands for High Performance Bulk Thermoelectrics*, Nature (London) **473**, 66 (2011).

[32] D. Kraemer, B. Poudel, H.-P. Feng, J. C. Caylor, B. Yu, X. Yan, Y. Ma, X. Wang, D. Wang, A. Muto, K. McEnaney, M. Chiesa, Z. Ren, and G. Chen, *High-Performance Flat-Panel Solar Thermoelectric Generators with High Thermal Concentration*, Nature Mater. **10**, 532 (2011).

[33] J. A. Woollam, H. Beale, and I. L. Spain, *Mobility in Single Crystal* Bi_2Se_3, Phys. Lett. A **41**, 319 (1972).

[34] H. Köhler and A. Fabricius, *Galvanomagnetic Properties of* Bi_2Se_3 *with Free Carrier Densities below* 5×10^{17} cm^{-3}, Phys. Status Solidi B **71**, 487 (1975).

[35] K. J. John, B. Pradeep, and E. Mathai, *Electrical Properties of Bismuth Selenide* (Bi_2Se_3) *Thin Films Prepared by Reactive Evaporation*, Solid State Commun. **85**, 879 (1993).

[36] X.-L. Li, K.-F. Cai, H. Li, L. Wang, and C.-W. Zhou, *Electrodeposition and Characterization of Thermoelectric*

Bi_2Se_3 *Thin Films*, Int. J. Minerals, Metallurgy and Materials **17**, 104 (2010).

[37] G. R. Hyde, H. A. Beale, I. L. Spain, and J. A. Woollam, *Electronic Properties of* Bi_2Se_3 *Crystals*, J. Phys. Chem. Solids **35**, 1719 (1974).

[38] N. P. Butch, K. Kirshenbaum, P. Syers, A. B. Sushkov, G. S. Jenkins, H. D. Drew, and J. Paglione, *Strong Surface Scattering in Ultrahigh-Mobility* Bi_2Se_3 *Topological Insulator Crystals*, Phys. Rev. B **81**, 241301 (2010).

[39] P. Janicek, C. Drasar, L. Benes, and P. Lost'ak, *Thermoelectric Properties of Tl-Doped* Bi_2Se_3 *Single Crystals*, Cryst. Res. Technol. **44**, 505 (2009).

[40] J. Navratil, J. Horak, T. Plechacek, S. Kamba, P. Lost'ak, J. S. Dyck, W. Chen, and C. Uher, *Conduction Band Splitting and Transport Properties of* Bi_2Se_3, J. Solid State Chem. **177**, 1704 (2004).

[41] H. Gobrecht and S. Seeck, *Dependence of the Effective Mass on the Charge Carrier Concentration in* Bi_2Se_3 (in German), Z. Phys. **222**, 93 (1969).

[42] U. Schlichting and K. H. Gobrecht, *The Mobility of Free Carriers in PbSe Crystals*, J. Phys. Chem. Solids **34**, 753 (1973).

[43] G. A. Slack, in *Solid State Physics*, edited by F. Seitz and D. Turnbull (Academic, New York, 1979), Vol. 34.